

## Spin Assignments of Low-Energy Resonances Using Polarized Neutrons and Polarized $\text{Sm}^{149}$ Nuclei\*

H. MARSHAK, HANS POSTMA,† V. L. SAILOR, F. J. SHORE,‡ AND C. A. REYNOLDS§

Brookhaven National Laboratory, Upton, New York

(Received June 20, 1962)

The spins of the four resonances at 0.0976, 0.87, 4.93, and 8.9 eV in  $\text{Sm}^{149}$  have been measured by using a monoenergetic polarized neutron beam incident on polarized samarium nuclei. By using one stage of adiabatic demagnetization, polycrystalline samples of samarium ethyl sulfate and samarium double nitrate were cooled to approximately 0.15°K. At this temperature and with the aid of an external magnetic field an appreciable polarization of the samarium nuclei is achieved by making use of the hfs coupling (Rose-Gorter method). The spin assignments for the above four resonances were all  $J = I + \frac{1}{2} = 4$ . The samarium nuclei in the double nitrate sample were found to be polarized in the same direction as in the ethyl sulfate sample. Measurements made on samarium metal at these low temperatures indicate that it is antiferromagnetic.

### I. INTRODUCTION

DURING the past decade there has been a large accumulation of data on the resonances which occur in slow-neutron cross sections.<sup>1</sup> These resonances correspond to excited states of the compound nucleus which are formed by  $l=0$  interactions, and which, therefore, are limited to a total angular momentum of  $J = I \pm \frac{1}{2}$ , where  $I$  is the spin of the target nucleus.

Despite the wealth of information about resonance parameters, the  $J$  values have been determined in relatively few cases. Several methods have been used for such determinations, but each of these suffers from some individual limitation which precludes its general application. In principle, an accurate measurement of the total and scattering cross section through the resonant region will yield the  $J$  value. Unfortunately, this method can only be used for those cases which have unusually large scattering cross sections, i.e., relatively strong resonances.<sup>2</sup>

There have been many attempts to infer the  $J$  value of the resonances by studying the capture  $\gamma$ -ray spectrum which is produced upon decay of the excited state.<sup>3-7</sup> In the initial work of this type, Kinsey and

Bartholomew<sup>3</sup> concluded that the negative-energy resonance ( $E_0 \approx -2$  eV) responsible for the thermal cross section in  $\text{Hg}^{199}$  ( $I = \frac{1}{2}$ ) was  $J = 0$ , since they could not detect a ground-state transition. Subsequently, Landon and Rae<sup>4</sup> determined that the spin of the next  $\text{Hg}^{199}$  resonance ( $E_0 = 34$  eV) was  $J = 1$  because the ground-state transition was observed. Additional measurements have yielded spin assignments for higher energy resonances in  $\text{Hg}^{199}$ ,<sup>5</sup> and the method has also been applied to other cases for which the target nucleus has a spin of  $\frac{1}{2}$ .<sup>6,7</sup> In cases for which the target spin  $I > \frac{1}{2}$ , measurements of the capture  $\gamma$ -ray spectrum can sometimes be used to assign spins of resonances.<sup>5</sup> In general, most of these techniques which depend upon the presence or absence of certain  $\gamma$ -ray transitions should be tested by using known spin assignments made by an unambiguous method.

Quite a different method which has been developed for making spin assignments of resonances involves the use of polarized neutrons and polarized target nuclei.<sup>8-10</sup> In this method, the transmission of the sample is measured at the resonant energy with the neutrons polarized parallel or antiparallel to the nuclear polarization. If the direction of the nuclear polarization is known, the spin assignment is straightforward and unambiguous. This method is not of general applicability since it requires elaborate equipment, and, at present, it is limited to resonances lying in the range from 0 to  $\sim 15$  eV; however, it can provide definite spin assignments for a limited number of cases, which can then be used as reference standards for other methods, e.g., one using capture  $\gamma$  rays.

In this paper we shall give results obtained on several resonances in  $\text{Sm}^{149}$ , using polarized neutrons and polarized nuclei, and describe some of the salient features of the experiment which were omitted in our preliminary

\* Work performed under the auspices of the U. S. Atomic Energy Commission.

† On leave of absence from the Kamerlingh Onnes Laboratory, Leiden, the Netherlands.

‡ Permanent address; Queens College, Flushing, New York.

§ Permanent address: University of Connecticut, Storrs, Connecticut.

<sup>1</sup> As a general reference summing up the work of many individuals, the reader is directed to *Neutron Cross Sections*, compiled by D. J. Hughes and R. B. Schwartz, Brookhaven National Laboratory Report BNL-325 (Superintendent of Documents, U. S. Government Printing Office, Washington 25, D. C. 1958), 2nd ed.

<sup>2</sup> B. N. Brockhouse, D. G. Hurst, and M. Bloom, *Phys. Rev.* **83**, 840 (1951); J. Tittman and C. Sheer, *ibid.* **83**, 746 (1951); B. N. Brockhouse, *Can. J. Phys.* **31**, 432 (1953); H. L. Foote, Jr., dissertation, University of Utah, 1954 (unpublished); R. E. Wood, *Phys. Rev.* **104**, 1425 (1956); J. A. Moore, *ibid.* **109**, 417 (1958).

<sup>3</sup> B. B. Kinsey and G. A. Bartholomew, *Can. J. Phys.* **31**, 1051 (1954).

<sup>4</sup> H. H. Landon and E. R. Rae, *Phys. Rev.* **107**, 1333 (1957).

<sup>5</sup> R. T. Carpenter and L. M. Bollinger, *Nuclear Phys.* **21**, 66 (1960).

<sup>6</sup> M. K. Brussel and R. L. Zimmerman, *Bull. Am. Phys. Soc.* **4**, 472 (1959).

<sup>7</sup> J. M. Julien, C. R. Corge, V. D. Heynh, S. U. Mirza, F. Nether, and J. Simic, *Bull. Am. Phys. Soc.* **4**, 472 (1959).

<sup>8</sup> S. Bernstein, L. D. Roberts, C. P. Stanford, J. W. T. Dabbs, and T. E. Stephenson, *Phys. Rev.* **94**, 1243 (1954); L. D. Roberts, S. Bernstein, J. W. T. Dabbs, and C. P. Stanford, *ibid.* **95**, 105 (1954); J. W. T. Dabbs, L. D. Roberts, and S. Bernstein, *ibid.* **98**, 1512 (1955).

<sup>9</sup> A. Stolovy, *Phys. Rev.* **118**, 211 (1960); *Bull. Am. Phys. Soc.* **5**, 294 (1960); *ibid.* **6**, 275 (1961).

<sup>10</sup> Hans Postma, H. Marshak, V. L. Sailor, F. J. Shore, and C. A. Reynolds, *Phys. Rev.* **126**, 979 (1962).

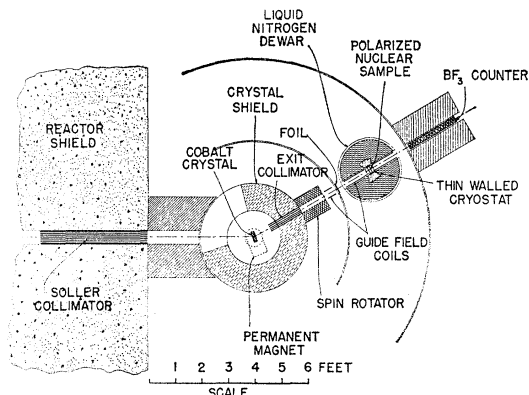


FIG. 1. Schematic view of the neutron polarization spectrometer and the cryostat for producing polarized nuclei.

publications.<sup>10,11</sup> In the last section we shall discuss a possible technique for deducing the spins of higher energy resonances by making use of some of the transitions observed in the capture  $\gamma$ -ray spectrum.

The resonances in the slow neutron cross section of  $\text{Sm}^{149}$  have been studied rather extensively.<sup>12,13</sup> Also, much work has been done on the  $\gamma$ -ray spectrum produced by the capture of thermal neutrons.<sup>14,15</sup> The work of Roberts *et al.*<sup>16</sup> illustrated that a reasonable polarization ( $\sim 11\%$ ) could be achieved at  $0.15^\circ\text{K}$  using the Rose-Gorter technique on the paramagnetic salt samarium ethyl sulfate. Using a thermal energy polarized neutron beam, they measured the spin of the first resonance at  $0.0976\text{ eV}$ , and found it to be  $I + \frac{1}{2} = 4$ . This agreed with the results of the scattering experiment of Brockhouse.<sup>17</sup> There are six other resonances below  $15\text{ eV}$ . By making use of a polarized neutron beam produced by Bragg reflection from a magnetized cobalt-iron single crystal and a polarized nuclear sample, we have measured the spin of three of the higher energy resonances at  $0.87$ ,  $4.93$ , and  $8.9\text{ eV}$ .

## II. APPARATUS

Figure 1 is a schematic view of the equipment. The neutron beam emerges from the BNL graphite reactor at the left of the drawing and passes through a Soller collimator in the reactor shield. It then impinges upon a cobalt-iron crystal which is mounted in a permanent magnet whose field is vertical. The value of the magnetic

induction in the crystal is about  $6000\text{ G}$ . The crystal serves the dual purpose of monochromatizing and polarizing the neutron beam. The diffracted neutrons are polarized parallel to the direction of the applied field of the crystal. The exit Soller collimator is magnetized in the same direction as the crystal magnet in order to maintain the beam polarization. As the neutrons pass from the collimator towards the target the magnetic field is rotated from the vertical to the horizontal by a series of small permanent magnets arranged in a spiral. The rotation can be changed from the "left" to the "right" by a mechanical reversal of the spiral. Thus, we can produce a neutron beam which is polarized parallel or antiparallel to the polarizing field at the nuclear sample. In the latter case, the direction of the guide field has to reverse somewhere along the beam path. This must be done rather abruptly in order to avoid depolarization of the beam. To achieve this reversal in a time short compared to the Larmor precession period, the neutron beam is passed through a thin aluminum foil carrying a large dc current.<sup>18</sup> The current direction is such that the resulting field is parallel to the neutron polarization on the incident side of the foil and antiparallel on the opposite side. Thus, the neutrons experience the reversal of the magnetic field in the time required for traversal of the foil. This time is very short compared to the Larmor period, and consequently the neutrons maintain their orientation in space despite the field reversal. The magnetic guide fields on each side of the foil have the appropriate di-

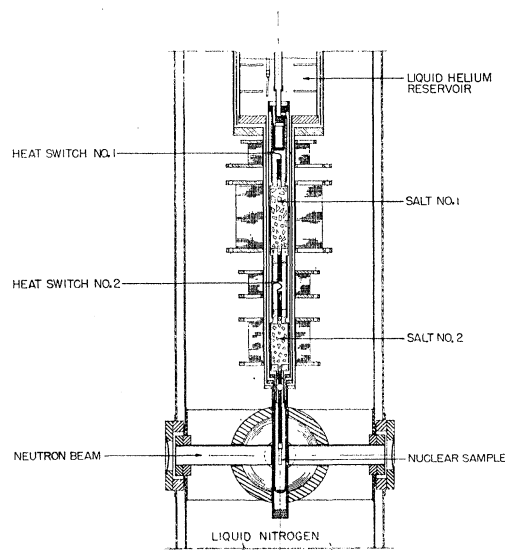


FIG. 2. Schematic view of the lower part of the cryostat showing the salt assembly and the nuclear sample. The polarizing iron core magnet, which is indicated by the shaded circular annulus, as well as the heat switch and salt magnets are all immersed in the liquid nitrogen.

<sup>11</sup> V. L. Sailor, R. I. Schermer, F. J. Shore, C. A. Reynolds, H. Marshak, and Hans Postma, *Phys. Rev.* **127**, 1124 (1962).

<sup>12</sup> H. Marshak and V. L. Sailor, *Phys. Rev.* **109**, 1219 (1958). The value for  $\sigma_0$  in Table I for the  $8.9\text{-eV}$  resonance should be  $22\,400 \pm 500\text{ b}$  instead of  $10\,200 \pm 300\text{ b}$ .

<sup>13</sup> F. B. Simpson and R. G. Fluharty, *Bull. Am. Phys. Soc.* **2**, 42 (1957).

<sup>14</sup> L. V. Groshev, A. M. Demidov, V. N. Lutsenka, and V. I. Pelekion, *Atlas of  $\gamma$ -Ray Spectra From Radiative Capture of Thermal Neutrons* (English translation, Pergamon Press, New York, 1959).

<sup>15</sup> R. K. Smither, *Bull. Am. Phys. Soc.* **7**, 316 (1962).

<sup>16</sup> L. D. Roberts, S. Bernstein, J. W. T. Dabbs, and C. P. Stanford, *Phys. Rev.* **95**, 105 (1954).

<sup>17</sup> B. N. Brockhouse, *Can. J. Phys.* **31**, 432 (1953).

<sup>18</sup> This method was originally suggested by J. W. T. Dabbs; J. W. T. Dabbs, L. D. Roberts, and S. Bernstein, Oak Ridge National Laboratory ORNL Document CF-55-5-126 (unpublished).

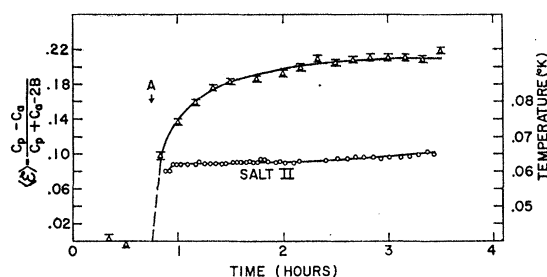


FIG. 3. The transmission effect,  $\langle 8 \rangle$ , vs time for the 0.0976-eV resonance in  $\text{Sm}^{149}$ . The nuclear sample was samarium ethyl sulfate. At time A the adiabatic demagnetization of the cooling (second) salt was completed. The warm-up curve for the cooling salt is shown, with the temperature scale at the right.

rection and strength to prevent depolarization. The guide fields extend into the gap of the magnet used for polarizing the nuclei, so that along the entire flight path the neutrons are in a magnetic field which is free from gradients that would cause depolarization.

The beam passes through several thin brass windows and thin layers of liquid nitrogen and liquid helium upon entering and leaving the cryostat, which reduce the beam intensity by approximately 20%. After leaving the cryostat, the neutrons are detected in a  $\text{BF}_3$  proportional counter. The arm of the spectrometer containing the cryostat can be rotated around the polarizing crystal on a track system so as to change the neutron energy by changing the Bragg angle. The  $\text{BF}_3$  counter and its shield can be removed and replaced by a small analyzing crystal and  $\text{BF}_3$  counter in order to measure the beam polarization by means of a second Bragg reflection.

The cryostat was designed for experiments in three different temperature regions. The highest temperature region is that of the liquid helium bath which, with our pumping system, ranges from  $\sim 0.95$  to  $4.2^\circ\text{K}$ . The other two regions, from  $\sim 0.05$  to  $0.95^\circ\text{K}$  and  $0.01$  to  $0.05^\circ\text{K}$ , are achieved by using one or two stages of magnetic cooling. The cryostat has a large reservoir for liquid helium and ample room for large paramagnetic salt assemblies so that these temperatures can be maintained for fairly long periods of time without recycling. On one filling of liquid helium, measurements can be carried out at  $0.95^\circ\text{K}$  for more than three days. Operating time for the other two temperature regions varies from a few hours to a day on one cooling cycle depending on the details in the construction of the sample assembly. The entire equipment will be described in greater detail elsewhere.<sup>19</sup>

The one stage assembly used in the samarium experiments is shown in Fig. 2. The first and second salts contain, respectively, 300 and 160 g of iron ammonium

alum. These salts consist of a polycrystalline mass grown on approximately 10 000 No. 40 B&S varnish-coated copper wires (e.g., Formvar) and are canned in vacuum tight annealed Lucite containers. The large number of wires give a contact area of about  $4.7 \times 10^3 \text{ cm}^2$  between the crystals and the copper for the first salt and about  $3.5 \times 10^3 \text{ cm}^2$  for the second salt. The Lucite containers are mechanically supported by thin cylinders of graphite.<sup>20</sup> The first salt is connected to the helium bath by a Pb heat switch  $0.35 \text{ mm}^2$  in cross section and 2.5 cm long. The second salt is joined to the first salt by a Pb heat switch of similar length by  $1.0 \text{ mm}^2$  in cross section. The solenoids for the magnetic cooling and the heat switches as well as the magnet for polarizing the nuclei are all immersed in the liquid nitrogen bath. Helium exchange gas is used only in the precooling from nitrogen temperatures to  $0.95^\circ\text{K}$ . The exchange gas is removed before the first magnetic cooling cycle and the heat of magnetization is transferred to the He bath through the heat switches. The salts are magnetized for 45 min and are then demagnetized in tandem, i.e., first salt I and then salt II. The first salt serves as a getter for any residual helium exchange gas in the adiabatic enclosure and as a guard salt to reduce the flow of heat from the bath to the second salt.

The temperatures of the cooling salts were determined by measuring the magnetic susceptibility using the ballistic method. The measurements were corrected for

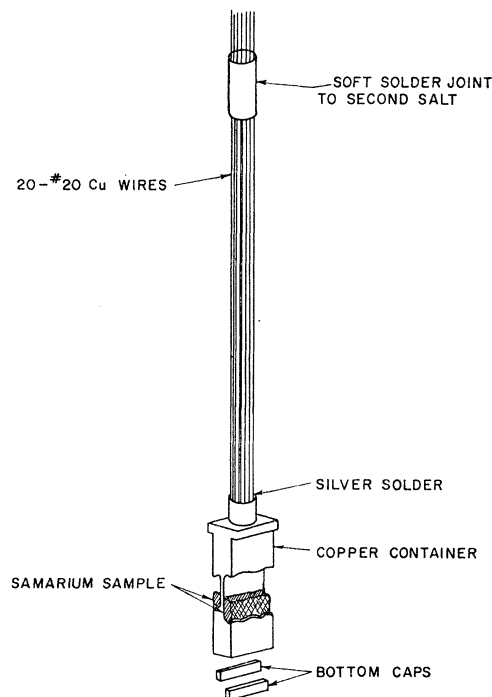


FIG. 4. A typical sample container which is used for the various samarium paramagnetic salts. The copper container is 2 cm wide, 5 cm long, and 0.4 cm thick.

<sup>19</sup> A complete description of the spectrometer and cryostat will be submitted to Rev. Sci. Instr. in the near future. Brief descriptions were given by H. Marshak, C. A. Reynolds, F. J. Shore, and V. L. Sailor, Bull. Am. Phys. Soc. 3, 17 (1958); and V. L. Sailor, H. Marshak, F. J. Shore, C. A. Reynolds, and H. Postma, *ibid.* 6, 275 (1961).

<sup>20</sup> F. J. Shore, V. L. Sailor, H. Marshak, and C. A. Reynolds, Rev. Sci. Instr. 31, 970 (1960).

the geometric shape of the salts and the magnetic temperatures thus obtained were converted to thermodynamic temperatures using the data of Cooke.<sup>21</sup> A typical warm-up curve for the second salt is shown in Fig. 3.

The samples of samarium ethyl sulfate and samarium double nitrate powder were packed in thin-walled copper containers, which were soft-soldered to the second salt, Fig. 4. After equilibrium is achieved between the sample and the second salt, the sample will be at a slightly higher temperature than the salt. This temperature difference will depend on the heat input into the sample and the thermal conductivity of the various parts connecting the sample to the salt. In Sec. VI the true temperature of the sample is estimated from the nuclear polarization.

### III. ANALYSIS

In making transmission measurements using a polarized neutron beam and a polarized nuclear sample, it is convenient to define a quantity called the transmission effect,  $\langle \mathcal{E} \rangle$ , as follows:

$$\langle \mathcal{E} \rangle = \frac{\langle \mathcal{T} \rangle_p - \langle \mathcal{T} \rangle_a}{\langle \mathcal{T} \rangle_p + \langle \mathcal{T} \rangle_a} \quad (1)$$

In the equation  $\langle \mathcal{T} \rangle_p$  and  $\langle \mathcal{T} \rangle_a$  are the transmissions of the beam through the sample for the cases in which the neutron polarizations are, respectively, parallel or antiparallel to the magnetic field applied to the sample. It has been shown<sup>10</sup> that the transmission of a polarized beam of slow neutrons passing through a polarized nuclear sample for the parallel orientation is given by

$$\langle \mathcal{T} \rangle_p = \int_0^\infty R(E' - E) e^{-N t \sigma_0 \psi(E', \eta)} \{ \cosh[N t \sigma_0 \psi(E', \eta) p] - f_n^0 \sinh[N t \sigma_0 \psi(E', \eta) p] \} dE' \quad (2)$$

The spectrometer resolution function,  $R(E' - E)$ , expresses the distribution of neutron energies in the incident beam,  $N$  is the density of target nuclei,  $t$  is the target thickness,  $\sigma_0 \psi(E', \eta)$  is the Doppler-broadened Breit-Wigner cross section,  $\eta$  is a quantity which involves the ratio of the Doppler width to the width of the resonance, and  $f_n^0$  is the incident neutron polarization. The information about the  $J$  value of the resonance is contained in the quantity  $p = \rho f_N$ , where  $\rho$  is a statistical weighting factor equal to  $I/(I+1)$  if the resonance is in the  $J = I + \frac{1}{2}$  state or  $-1$  for the  $J = I - \frac{1}{2}$  state, and  $f_N$  is the nuclear polarization. We have assumed here that there is no depolarization of the neutron beam due to magnetic effects in passing through the sample (see reference 10 for the case in which depolarization does occur).

The equation for  $\langle \mathcal{T} \rangle_a$  is similar to Eq. (2) except that  $f_n^0$  is replaced by  $-\phi f_n^0$ , where  $\phi$  is efficiency for reversing the neutron polarization from the parallel

orientation to the antiparallel. Substituting the appropriate expressions into Eq. (1), and for  $\phi$  close to unity, we obtain

$$\langle \mathcal{E} \rangle = -f_n^0 \frac{(1+\phi)}{2} \frac{\int_0^\infty R(E' - E) e^{-N t \sigma_0 \psi(E', \eta)} \sinh[N t \sigma_0 \psi(E', \eta) p] dE'}{\int_0^\infty R(E' - E) e^{-N t \sigma_0 \psi(E', \eta)} \cosh[N t \sigma_0 \psi(E', \eta) p] dE'} \quad (3)$$

This expression must be solved numerically. When there is no resolution correction, this equation reduces to the simple formula

$$\mathcal{E} = -f_n^0 [(1+\phi)/2] \tanh[N t \sigma_0 \psi(E, \eta) p] \quad (4)$$

If  $C_p$  and  $C_a$  are the counting rates for the parallel and antiparallel orientations,  $C_0$  the open-beam counting rate, and  $B$  the background counting rate, then by definition

$$\langle \mathcal{T} \rangle_p = (C_p - B)/(C_0 - B), \quad \text{and} \quad \langle \mathcal{T} \rangle_a = (C_a - B)/(C_0 - B) \quad (5)$$

If  $C_0$  and  $B$  remain constant during the measurement of  $\langle \mathcal{E} \rangle$ , then Eq. (1) can be written:

$$\langle \mathcal{E} \rangle = (C_p - C_a)/(C_p + C_a - 2B) \quad (6)$$

It is obvious that an observation of the directional change of the counting rate for the parallel case compared to the antiparallel case is sufficient to determine the spin of the resonance level. The determination, of course, depends upon knowing whether the nuclear spins are polarized parallel or antiparallel to the external applied magnetic field. In order to relate the magnitude of  $\langle \mathcal{E} \rangle$  to the nuclear polarization, one must use Eq. (3). From the value for the nuclear polarization thus obtained, a sample temperature can be deduced by using one of the appropriate expressions which are given in Sec. V.

In order to calculate  $f_N$  from Eq. (3), various other quantities in the expression must be deduced. The values of  $f_n^0$  and  $\phi$  are measured directly by means of a Bragg reflection from cobalt-iron crystal which is mounted in place of the  $BF_3$  counter. The Doppler broadened Breit-Wigner cross section  $\sigma_0 \psi(E, \eta)$  can be calculated if the parameters of the resonance and the Debye temperature are known. The quantity  $\rho$  follows, of course, from the sign of the transmission effect.

### IV. NEUTRON CROSS SECTION OF SAMARIUM BELOW 15 eV

The resonance structure below 15 eV in the neutron cross section of the stable isotopes of samarium has been

<sup>21</sup> A. H. Cooke, Proc. Phys. Soc. (London) **A62**, 269 (1949).

thoroughly studied.<sup>12,13,22,23</sup> Resonances occur in  $\text{Sm}^{147}$  at 3.4 eV, in  $\text{Sm}^{149}$  at 0.0976, 0.87, 4.93, 6.45, 8.9, 12.2, and 14.8 eV, and in  $\text{Sm}^{152}$  at 8.04. Except for the resonances at 12.2 and 14.8 eV in  $\text{Sm}^{149}$ , the parameters ( $\Gamma_\gamma$ ,  $\Gamma_n$ , and  $\sigma_0$ ) for all the levels have been determined with good accuracy. Since the resonances differ widely in strength, and since the unusually strong resonance in  $\text{Sm}^{152}$  at 8.04 eV almost obscures the two resonances in  $\text{Sm}^{149}$  at 6.45 and 8.9 eV, a sample enriched in  $\text{Sm}^{149}$  and highly depleted in  $\text{Sm}^{152}$  is required for our measurements. This sample could also be used to measure the spin of the 4.93-eV resonance.

No special sample was prepared which would permit an adequate study of the spin of the 3.4-eV resonance in  $\text{Sm}^{147}$ .  $\text{Sm}^{152}$  is an even-even nucleus, it has a spin of zero; hence, the spin of the 8.04-eV level must be  $J=\frac{1}{2}$ .

Our spectrometer resolution was insufficient to resolve the 12.2- and 14.8-eV resonances, so the spins could not be determined for these levels. The 6.45-eV resonance proved to be too weak to yield a definite result.

## V. NUCLEAR POLARIZATION

The nuclear polarization for a nuclear spin system in thermodynamic equilibrium is given by the following expression<sup>24</sup>:

$$f_N = \frac{\text{Tr}[I_z \exp(\mathcal{H}/kT)]}{I \text{Tr}[\exp(\mathcal{H}/kT)]}, \quad (7)$$

where  $I_z$  is the  $z$  component of the nuclear spin  $I$ , and  $\mathcal{H}$  is the Hamiltonian of the system. Thus, in order to calculate  $f_N$  the Hamiltonian of the system has to be known.

The magnetic properties of rare earth salts such as the ethyl sulfates,  $M(\text{C}_2\text{H}_5\text{SO}_4)_3 \cdot 9\text{H}_2\text{O}$ , and the double nitrates,  $M_2\text{Mg}_3(\text{NO}_3)_{12} \cdot 24\text{H}_2\text{O}$ , have been extensively studied both experimentally and theoretically. The spin Hamiltonians, which describe the properties of the ground states of these ions, are well understood in terms of the trigonal electric crystal field parameters. In case of ions with double degeneracy (that is, for an odd number of  $4f$  electrons), the paramagnetic resonance data can be represented by the following spin Hamiltonian  $\mathcal{H}$  with the effective spin operator  $\mathbf{S}'$ :

$$\mathcal{H} = g_{11}\beta H_x S'_x + g_{12}\beta (H_x S'_x + H_y S'_y) + AS'_z I_z + B(S'_x I_x + S'_y I_y) + \mathcal{H}', \quad (8)$$

where the first two terms describe the Zeeman splitting and the second two terms the magnetic hyperfine interaction.  $I$  is the nuclear spin operator.  $\mathcal{H}'$  includes the remaining interactions such as spin-spin, quadrupole, and direct coupling of the nuclear magnetic moment to

TABLE I. Paramagnetic resonance data for samarium ethyl sulfate and samarium double nitrate.

Sample	$g_{11}$	$g_{12}$	$A/k$ (°K)	$B/k$ (°K)
Samarium ethyl sulfate <sup>a</sup> (relative to $\text{Sm}^{149}$ )	+0.596	+0.604	-0.0070	-0.0293
Samarium double nitrate <sup>b</sup> (relative to $\text{Sm}^{149}$ )	-0.76	0.40	+0.041	$0 > B/k > -0.0157$

<sup>a</sup> The magnitudes are from reference 25, whereas the signs are from references 26 and 27.

<sup>b</sup> The magnitudes are from reference 28, whereas the signs are from reference 29.

the external field  $\mathbf{H}$ . The terms included in  $\mathcal{H}'$  are usually small compared to the terms which are explicitly written down in the above formula.

## A. Samarium Ethyl Sulfate

The values of the various constants in the spin Hamiltonian for samarium ethyl sulfate derived by paramagnetic resonance experiments<sup>25</sup> at 4.2°K are given in Table I. The values for  $g_{11}$  and  $g_{12}$  are nearly equal; thus the spin Hamiltonian can in good approximation be rewritten as

$$\mathcal{H} = g\beta \mathbf{H} \cdot \mathbf{S} + AS_z I_z + B(S_x I_x + S_y I_y). \quad (9)$$

In first order the electronic ground state is a  $J_z = \pm \frac{1}{2}$  doublet with  $J = \frac{5}{2}$ . Introducing a small admixture from the first excited state with  $J = \frac{7}{2}$ , Elliott and Stevens<sup>26</sup> could explain the isotropy of the  $g$  factor. With the same amount of admixture the calculated ratio  $A/B$  is equal to the experimental value 0.24. The sign of the nuclear magnetic moment of  $\text{Sm}^{149}$  is deduced by Murakawa to be negative.<sup>27</sup> Hence  $\text{Sm}^{149}$  polarizes antiparallel to the applied external field in case of samarium ethyl sulfate; i.e.,  $f_N < 0$ .

The nuclear polarization for a powdered sample of samarium ethyl sulfate is, to first approximation, given by<sup>16</sup>

$$f_N = \frac{I+1}{6kT} \left( \frac{A+2B}{3} \right) \tanh \frac{g\beta H}{2kT}. \quad (10)$$

For the case of  $\text{Sm}^{149}$  ethyl sulfate this reduces to

$$f_N = -(0.0165/T) \tanh(2.02 \times 10^{-5} H/T). \quad (11)$$

Thus, for example, a temperature of 0.1°K and a value of  $H = 10$  kOe would produce a nuclear polarization of 15.9%.

## B. Samarium Double Nitrate

Paramagnetic resonance measurements<sup>28</sup> have also been made on samarium double nitrate at 4.2°K. The

<sup>22</sup> N. J. Pattenden, H. J. Hay, and A. H. Baston, A.E.R.E., NP/M-87, 1958 (unpublished).

<sup>23</sup> Brother A. Bernabei, L. B. Borst, and V. L. Sailor, Nuclear Sci. and Eng. **12**, 63 (1962).

<sup>24</sup> A. Simon, M. E. Rose, and J. M. Jauch, Phys. Rev. **84**, 1155 (1951).

<sup>25</sup> G. S. Boyle and H. E. D. Scovil, Proc. Phys. Soc. (London) **A65**, 386 (1952).

<sup>26</sup> R. J. Elliott and K. W. H. Stevens, Proc. Roy. Soc. (London) **A219**, 387 (1953).

<sup>27</sup> Kiyoshi Murakawa, Phys. Rev. **93**, 1232 (1954).

<sup>28</sup> A. H. Cooke and H. J. Dreffus, Proc. Roy. Soc. (London) **A229**, 407 (1955).

constants of the spin Hamiltonian are also given in Table I. A theoretical treatment is given by Judd.<sup>29</sup> He obtained a reasonable agreement between the experimental and theoretical values of  $g_{11}$ ,  $g_{\perp}$ , and  $A$ , while the calculated value of  $B$  is smaller than the upper limit given by the experiment.

The inequality of the  $g$  values has to be taken into consideration in obtaining the average nuclear polarization for a powdered sample. The nuclear polarization along the field direction for crystallites, whose  $c$  axis makes an angle  $\theta$  with the field direction, is approximately<sup>30</sup>

$$f_N = \frac{I+1}{6kT} \left[ \frac{Ag_{11} \cos^2\theta + Bg_{\perp} \sin^2\theta}{g} \right] \tanh \frac{g\beta H}{2kT}, \quad (12)$$

where

$$g = +[g_{11}^2 \cos^2\theta + g_{\perp}^2 \sin^2\theta]^{1/2}.$$

Equation (12) averaged over a random angular distribution of  $c$  axis in a powder sample becomes

$$f_N = [(I+1)/6kT] [Ag_{11}R_2 + Bg_{\perp}(R_0 - R_2)], \quad (13)$$

where

$$R_2 = \int_0^{\pi/2} g^{-1} \tanh\left(\frac{g\beta H}{2kT}\right) \cos^2\theta \sin\theta \, d\theta,$$

$$R_0 = \int_0^{\pi/2} g^{-1} \tanh\left(\frac{g\beta H}{2kT}\right) \sin\theta \, d\theta.$$

The integrals  $R_0$  and  $R_2$  must be numerically integrated in order to calculate the average nuclear polarization.

Since both  $Ag_{11}$  and  $Bg_{\perp}$  have negative signs, the nuclear polarization is expected to be negative; i.e., the  $\text{Sm}^{149}$  nuclei are polarized antiparallel to the applied field in the case of samarium double nitrate. Thus samarium double nitrate and samarium ethyl sulfate should exhibit transmission effects of the same sign.

## VI. EXPERIMENTAL RESULTS

Three types of polycrystalline samples were used during the experiments, namely, samarium ethyl sulfate  $[\text{Sm}(\text{C}_2\text{H}_5\text{SO}_4)_3 \cdot 9\text{D}_2\text{O}]$ , samarium double nitrate  $[\text{Sm}_2\text{Mg}_3(\text{NO}_3)_{12} \cdot 24\text{D}_2\text{O}]$ , and samarium metal. The salts were prepared from  $\text{Sm}_2\text{O}_3$ . Both the oxide and the metal had a purity of 99.9%.<sup>31</sup> In both salts the water of crystallization was replaced by  $\text{D}_2\text{O}$  to reduce the neutron scattering of the sample. The samarium ethyl sulfate was studied because the measurements could be compared to a previous experiment using polarized thermal neutrons.<sup>16</sup> The samarium double nitrate offered

<sup>29</sup> B. R. Judd, Proc. Roy. Soc. (London) **A232**, 458 (1955). Apparently the value listed for  $A$  on p. 471 should be positive instead of negative. This can be verified by inserting the constants into the equation for  $A$ , and remembering that the magnetic moment for  $\text{Sm}^{149}$  is negative.

<sup>30</sup> R. I. Schermer (private communication).

<sup>31</sup> These samples were obtained from the Lindsay Chemical Division, American Potash and Chemical Corporation.

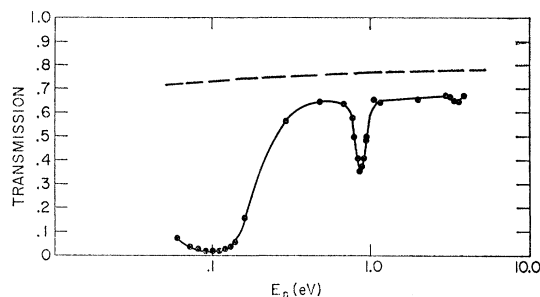


FIG. 5. The transmission of samarium ethyl sulfate vs neutron energy. The dashed curve is the calculated transmission for the deuterated ethyl sulfate component.

certain advantages over the samarium ethyl sulfate in that all the hydrogen could easily be replaced by deuterium. The deuterated salt then has only about 270 b of additional cross section per samarium atom due to the rest of the molecule, as compared to about 480 b of additional cross section per samarium atom for deuterated samarium ethyl sulfate. The reduction of background cross section is especially important for the higher energy resonances. In addition, it is interesting to compare the results for the samarium double nitrate with those of samarium ethyl sulfate.

### A. Samarium Ethyl Sulfate

The crystals of samarium ethyl sulfate were ground to a coarse powder of particle size between 0.1 and 0.5 mm. The sample thickness,  $Nt$ , in terms of  $\text{Sm}^{149}$  atoms was  $0.749 \times 10^{20}/\text{cm}^2$ . This was determined by measuring both the size and weight of the sample. The value of  $Nt$  was checked by measuring the known cross section at 0.146 eV, where the resolution and Doppler corrections are negligible. The transmission as a function of neutron energy was measured at room temperature before the sample was attached to the salt assembly. The results of these measurements, which were obtained using the (111) planes of the cobalt-iron crystal, are shown in Fig. 5. The first two transmission dips are due to the first two resonances in  $\text{Sm}^{149}$  at 0.0976 and 0.87 eV, whereas the third smaller dip is the 3.4-eV resonance in  $\text{Sm}^{147}$ . The sample was designed to be of optimum thickness for the second resonance. Since this criterion yielded a fairly thick sample for measuring the transmission effect at the peak (0.0976 eV) of the first resonance, measurements were made at a slightly higher energy (0.146 eV).

The transmission effect,  $\langle \mathcal{E} \rangle$ , was measured by recording counts for 4.7-min intervals with the neutrons polarized parallel to the applied field (10 kOe) at the nuclear sample. The direction of neutron polarization was then reversed to the antiparallel orientation during the next 0.3-min interval. Data were again recorded for a 4.7-min interval in the antiparallel orientation and so on. The background counting rate  $B$  was obtained by turning the cobalt-iron crystal  $2^\circ$  off the Bragg angle.

TABLE II. Summary of the results of polarization measurements on samarium. The measured effect  $\langle \mathcal{E} \rangle$  after thermal equilibrium was achieved is given in the third column. For  $\text{Sm}^{149}$ ,  $I=7/2$ ; hence, the spin of the compound state can be  $J=3$  or 4. All four resonances which could be measured were found to be  $J=4$ . The nuclear polarization  $f_N$  was calculated from  $\langle \mathcal{E} \rangle$  using Eq. (3), which takes into account spectrometer resolution and Doppler broadening. The fifth column gives the temperature calculated from the nuclear polarization, and the last column gives the temperature of the second salt.

Sample	Resonance energy $E_0$ (eV)	Measured transmission effect $\langle \mathcal{E} \rangle$ (%)	J value	Calculated nuclear polarization $f_N$ (%)	$\bar{T}$ (calculated from $f_N$ ) ( $^{\circ}\text{K}$ )	$\bar{T}_{II}$ (measured) ( $^{\circ}\text{K}$ )
$\text{Sm}(\text{C}_2\text{H}_3\text{SO}_4)_8 \cdot 9\text{D}_2\text{O}$	0.0976 <sup>a</sup>	$+20.7 \pm 0.1$	4 <sup>c</sup>	-13.2	0.12	0.062
	0.870	$+4.6 \pm 0.3$	4	-9.9	0.15	0.073
$\text{Sm}_2\text{Mg}_2(\text{NO}_3)_{12} \cdot 24\text{D}_2\text{O}$	0.0976	$+15.2 \pm 0.1$	4	-9.4	0.16	0.060
	0.870	$+4.6 \pm 0.3$	4	-9.9	0.15	0.064
$\text{Sm}_2^{149}\text{Mg}_2(\text{NO}_3)_{12} \cdot 24\text{D}_2\text{O}$	4.93	$+1.23 \pm 0.25$	4	-15.4	0.11	0.058
	6.45	$-0.19 \pm 0.24$	...	...	...	...
	8.9	$+0.83 \pm 0.35$	4	-18.2	0.10	0.050
Sm metal	0.0976 <sup>b</sup>	$-0.00 \pm 0.12$		Antiferromagnetic		

<sup>a</sup> These data were taken at a neutron energy of 0.146 eV.

<sup>b</sup> These data were taken at a neutron energy of 0.250 eV.

<sup>c</sup> This result agrees with references 16 and 17.

The transmission effect was also measured at  $0.95^{\circ}\text{K}$  and during the magnetization of the salts to demonstrate that  $\langle \mathcal{E} \rangle$  was zero when the sample was "warm." The results of each pair of counts ( $C_p$  and  $C_a$ ) in a 10-min interval were used to calculate  $\langle \mathcal{E} \rangle$ . The statistical uncertainty in  $\langle \mathcal{E} \rangle$  was calculated from the total counts accumulated in each cycle.

In Fig. 3 the results of a typical demagnetization are presented. In the figure, the salts were magnetized from time zero to time A (45 min) and then demagnetized in tandem. The transmission effect measured during this time was zero within the statistical uncertainty. The first point after time A was  $\langle \mathcal{E} \rangle = +9.8 \pm 0.3\%$ . The positive sign indicates that the spin of the first resonance is  $I + \frac{1}{2} = 4$ . This follows since we know that the nuclei are polarized antiparallel to the applied field. This assignment is in agreement with previous results.<sup>16,17</sup>

Since the sample is in the form of a powder, the heat transport from the sample is rather poor and an equilibrium temperature should be achieved only after some time delay. From Fig. 3 we see that this equilibrium time is approximately 90 min, at which time the transmission effect reached a constant value of  $+20.6 \pm 0.3\%$ . The corrected temperature of the second salt,  $\bar{T}_{II}$ , at this time was  $0.063^{\circ}\text{K}$ , and during the next 80 min  $\bar{T}_{II}$  increased by only  $0.002^{\circ}\text{K}$ . The average value of  $\langle \mathcal{E} \rangle$  and that of  $\bar{T}_{II}$  during the 80-min interval after equilibrium are given in the first line of Table II. Results for the other resonances obtained in a similar manner are also shown in Table II.

At each resonance Eq. (3) was used to calculate  $f_N$  from the measured value of  $\langle \mathcal{E} \rangle$ . In these calculations we have assumed that depolarization of the beam due to the sample is negligible because of the isotropy of the  $g$  factor and because of the strong polarizing field. This assumption appears reasonable if one makes a comparison with holmium ethyl sulfate, which has an extremely anisotropic  $g$  factor, and yet exhibits negligible depolarization for low-energy neutrons if the polarizing fields are 10 kOe or greater.<sup>10</sup> The polarization of the incident neutron beam  $f_n^0$  and the efficiency for revers-

ing the neutron polarization were measured by a Bragg reflection from a second cobalt-iron crystal. The measured values were  $f_n^0 = 0.95$  and  $\phi = 0.98$ . The uncertainty in these values is of the order of a few percent.

The value of  $f_N$  in Table II can be used to calculate the average temperature of the nuclear sample. Using Eq. (11), we find that  $\bar{T}(\text{calculated}) = 0.12^{\circ}\text{K}$ . The temperature difference between the nuclear sample and the second salt is probably due to the heat input arising from eddy currents in the sample container resulting from small oscillations of the sample in the large gradient of the gap of our polarizing magnet.

The necessity for making corrections for spectrometer resolution and Doppler broadening must be emphasized. If these corrections are neglected, the value of  $f_N$  calculated from the measured  $\langle \mathcal{E} \rangle$  is in error. The discrepancy, of course, depends on the energy of the resonance, becoming more serious as the energy increases. To illustrate the magnitude of the error, let us compare values of  $f_N$  calculated with Eq. (3) with those calculated from Eq. (4) which neglects resolution. As would be expected for the 0.0976-eV resonance the difference is small,  $f_N = 13.2\%$  [from Eq. (3)] compared to  $f_N = 12.9\%$  [from Eq. (4)], since at such a low energy the spectrometer resolution has little effect. However, at 8.9 eV the two values are, respectively, 18.2% (with correction) compared to 9.3% (without correction).

For the Doppler correction the Debye temperature of samarium ethyl sulfate is not known. The value used was  $\Theta \cong 150^{\circ}\text{K}$ .<sup>32</sup> In the calculations, we tested the sensitivity of the corrections to the Debye temperature and found that variation of  $\Theta$  produced negligible changes in the corrected value in this energy range.

Since the sample is a paramagnetic salt, a partial demagnetization will further reduce its temperature, and thus increase the nuclear polarization. This effect was previously discussed by Roberts *et al.*,<sup>16</sup> who concluded that an optimum value for the nuclear polarization,  $f_N'$ , obtained with the optimum final field, can be cal-

<sup>32</sup> K. Gschneidner, *Rare Earth Alloys* (D. Van Nostrand Company, Inc., Princeton, New Jersey, 1961), p. 58.

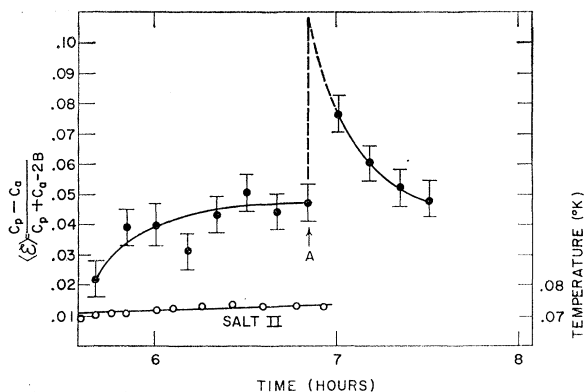


FIG. 6. The transmission effect vs time for the 0.87-eV resonance in  $\text{Sm}^{149}$ . This is a continuation of the same cooling cycle as shown in Fig. 3. At time  $A$  the polarizing field at the nuclear sample was reduced from 10 to 2 kOe. This partial demagnetization enhanced the nuclear polarization.

culated from the following equation:

$$f_N' = -\frac{1}{6} \frac{S(I+1)}{[I(I+1)]^{1/2}} \frac{g\beta H_i}{kT_i} \tanh \frac{g\beta H_i}{2kT_i}, \quad (14)$$

where the subscript  $i$  refers to the initial conditions before the partial demagnetization. The optimum final field, which must be large enough to saturate the electronic moments,<sup>33</sup> has to be determined experimentally in the absence of complete thermodynamic data specifying the entropy of the salt as a function of  $H$  and  $T$ . Substituting  $H_i = 10$  kOe,  $T_i = 0.15^\circ\text{K}$ , and the other constants into Eq. (14), we obtain  $f_N' = 22\%$ . Using Eq. (3), this corresponds to a value of  $\langle\mathcal{E}\rangle = 13.8\%$  for the 0.87-eV resonance.

A partial demagnetization in which the field was reduced from 10 to 2 kOe was performed at the 0.87-eV resonance. These results are shown in Fig. 6, where  $A$  indicates the time of demagnetization. The nuclear polarization and hence  $\langle\mathcal{E}\rangle$  would be a maximum at time  $A$ , then decrease, due to the sample warming up. The value of the transmission effect at time  $A$ , which is obtained by extrapolation, is 10.5%. This is in fairly good agreement with the calculated value above when one considers that the optimum value of  $H_f$  is probably lower than 2 kOe. The effect of partial demagnetization on the nuclear sample was also investigated at the first resonance where the transmission effect is much larger. This result for the enhancement of the nuclear polarization was also in good agreement with the calculated value using Eq. (14). In order to exploit the partial demagnetization it would be necessary to mount a heat switch between the second salt and the sample. This would reduce the heat leak from the second salt to the sample and will give a substantially longer measuring period after the partial demagnetization.

<sup>33</sup> J. W. T. Dabbs and L. D. Roberts, Phys. Rev. **95**, 970 (1954).

## B. Samarium Double Nitrate

The measurements of  $\langle\mathcal{E}\rangle$  using samarium double nitrate were carried out at 0.146 eV, Fig. 7, using the same salt assembly as before. The value of  $Nt$  was  $0.748 \times 10^{20}$   $\text{Sm}^{149}$  nuclei/cm<sup>2</sup>, which is almost the same as that of the Sm ethyl sulfate. As in the ethyl sulfate the Sm nuclei are polarized antiparallel to the applied field, and, hence, the transmission effect is expected to have the same sign. Indeed a positive value of  $\langle\mathcal{E}\rangle$  was observed. The magnitude of  $\langle\mathcal{E}\rangle$  was obtained by averaging the data after thermal equilibrium. The time for thermal equilibrium was approximately the same as for samarium ethyl sulfate. From the measured  $\langle\mathcal{E}\rangle$  the value of  $f_N$  was obtained. This result is given in Table II. In order to obtain the average sample temperature from  $f_N$ , Eq. (13) was used. The magnitudes for  $A$ ,  $B$  (maximum value),  $g_{11}$ , and  $g_1$  used were those given in Table I. The value of  $\bar{T}$  (calculated) was  $0.16^\circ\text{K}$ , which is in fairly good agreement with the temperatures calculated for the samarium ethyl sulfate sample. If the magnitude of the hyperfine coupling constant  $B$  were smaller, the agreement would be somewhat better.

A partial demagnetization of the double nitrate sample was also performed by reducing the field from 10 to 2 kOe. The result is shown in Fig. 7, where  $B$  represents the time of demagnetization. Extrapolating back to time  $B$  gives  $\langle\mathcal{E}\rangle \approx 0$ . The effect then grows back in and is about 50% as large as before. This value of  $\langle\mathcal{E}\rangle$  ( $\sim 8.0\%$ ) yields a value of 4.9% for  $f_N$ . From this value for the nuclear polarization and the magnetic field value of 2 kOe, we calculate an average sample temperature of  $0.17^\circ\text{K}$ . This agrees well with the value obtained at 10 kOe.

We are unable to explain why the partial demagnetization did not enhance the nuclear polarization. Since  $\langle\mathcal{E}\rangle \approx 0$  at time  $B$ , we would suspect that heat was generated in the sample which masked any cooling due to the demagnetization. Obviously, some heat is generated by eddy currents induced in the copper sample con-

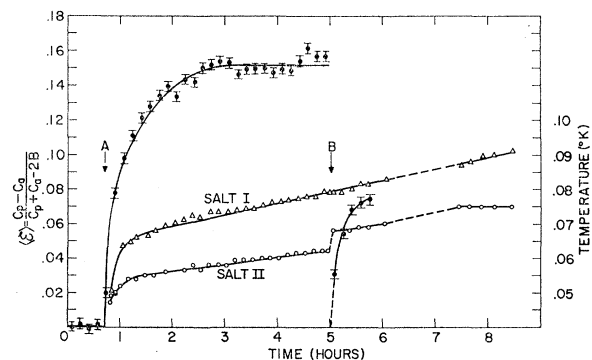


FIG. 7. The transmission effect vs time for the 0.0976-eV resonance in  $\text{Sm}^{149}$ . The sample was samarium double nitrate. The warm-up curves for salts I and II are shown. At time  $B$  the polarizing field at the sample was reduced from 10 to 2 kOe, and failed to enhance the nuclear polarization.



tainer when the magnetic field is reduced. However, the specific heat due to the hyperfine coupling is about the same for both salts, and therefore one would suspect that both salts would absorb this eddy current heating about the same. Since very little is known about the magnetic properties of samarium double nitrate at these low temperatures (e.g., a possible magnetic transition), no definite conclusion can be made at this time.

The transmission effect was also measured at the 0.87-eV resonance and the results are given in Table II.

### C. Samarium-149 Double Nitrate

Samarium double nitrate was prepared from an enriched (81.46%)  $\text{Sm}^{149}$  sample. The thickness of this sample ( $3.6 \times 10^{20}$   $\text{Sm}^{149}$  nuclei/cm<sup>2</sup>) was limited by the amount of  $\text{Sm}^{149}$  that was available. Preliminary calculations indicated that the transmission effects at the 4.93- and 8.9-eV resonances would be small ( $\sim 1\%$ ). Since the 6.45-eV resonance is much weaker, a much thicker separated isotope sample is needed.

The transmission effect was measured at the 4.93-, 6.45-, and 8.9-eV resonances using the Co(220) planes. These planes were used rather than the Co(111) planes since for the same energy setting they yield a larger Bragg angle, thus better resolution. This larger Bragg angle also reduces the part of our background which is due to the scattering of the direct beam. However, we lose some intensity for this reflection as well as polarization. The neutron polarization for the Co(220) planes is estimated to be 0.76 and the flipping efficiency is almost unity for these energies. The results of these measurements are given in Table II. The values for  $\bar{T}$ (calculated) and  $\bar{T}$ (measured) are also given in this table. The nuclear polarizations were somewhat larger (hence the average calculated temperature lower) than our previous results for the lower energy resonances. This discrepancy is probably due to an uncertainty in our sample thickness since the correction for resolution and Doppler broadening are very sensitive to this quantity for these resonances. The spins of the resonance levels at 4.93 and 8.9 eV were found to be 4. Measurements made at the 6.45-eV resonance yielded no definite spin assignment. For comparison with the measurements using the normal samarium samples the transmission effect was remeasured at the 0.87-eV resonance, and the result was in agreement with our previous conclusions.

### D. Samarium Metal

Magnetic susceptibility measurements<sup>34</sup> made on samarium metal indicate an anomaly at 14.8°K. Specific heat measurements<sup>35</sup> indicate a peak at approximately the same temperature. It has been suggested by Lock<sup>34</sup> that this is a Néel point; i.e., samarium metal is antiferromagnetic below this temperature. Recent specific

heat measurements<sup>36</sup> made at lower temperatures in the region of the hyperfine specific heat anomaly indicate that the effective field at the samarium nucleus is  $3.3 \times 10^6$  Oe. If samarium metal were not antiferromagnetic below 14.8°K, a large nuclear polarization would occur and hence a large transmission effect would be observed.

A sample of samarium metal 0.71 mm thick was used to measure the transmission effect at low temperatures. The sample was prepared by spraying with molten copper and then soldering it between two sheets of copper. The solder used was a high purity tin-lead eutectic which has a low neutron cross section. The sample was attached to the same salt assembly that was used for the separated isotope experiment. The temperature of the sample was estimated from previous work to be approximately 0.1°K. The magnetic field of the polarizing magnet was 10 kOe. The transmission effect was measured at an energy of 0.25 eV. At this energy almost all of the cross section is due to the 0.0976-eV resonance. The value obtained for the transmission effect (see Table II) indicates that the nuclear polarization is zero. One can thus conclude that samarium metal is antiferromagnetic at these temperatures.

The depolarization of the neutron beam was measured at 4.2°K. The energy of the neutron beam was 0.198 eV, and the polarizing field was 17 kOe. These results showed no depolarization of the neutron beam in passing through the samarium sample. This is consistent with the interpretation that samarium metal is antiferromagnetic below 14.8°K.

## VII. CONCLUSIONS

The results of the spin assignments for four of the five lowest resonances in  $\text{Sm}^{149}$  were all  $J = I + \frac{1}{2} = 4$ . These four resonances have radiation widths which are almost identical.<sup>12</sup> However, one should not attach too much significance to this fact until more data on many other resonances are obtained.

The low-energy capture  $\gamma$ -ray spectrum for the first three resonances has been measured.<sup>12,37</sup> The results indicate that there are no appreciable differences in the absolute intensities for the transitions from the first excited state to the ground state (330 keV) and from the second to the first excited states (440 keV) for these three resonances. It is much more interesting to look at the high-energy  $\gamma$ -ray transitions at the various neutron resonances. In particular, assuming sufficient  $\gamma$ -ray intensity, it would be worthwhile to look for the branching ratio of the two radiations from the capturing state to the first and second excited states, Fig. 8. In the case of a  $3^-$  capturing state, these two radiations are expected to occur since both are  $E1$  transitions. In the case of a  $4^-$  capturing state the transition to the first excited state ( $2^+$ ) will be suppressed because of its  $M2$  character;

<sup>36</sup> O. V. Lounasmaa, *Bull. Am. Phys. Soc.* **7**, 55 (1962).

<sup>37</sup> C. A. Fenstermacher, R. G. Bennett, A. E. Walters, C. K. Bockelman, and H. L. Schultz, *Phys. Rev.* **107**, 1650 (1957).

<sup>34</sup> J. M. Lock, *Proc. Phys. Soc. (London)* **B70**, 566 (1957).

<sup>35</sup> L. M. Roberts, *Proc. Phys. Soc. (London)* **B70**, 435 (1957).

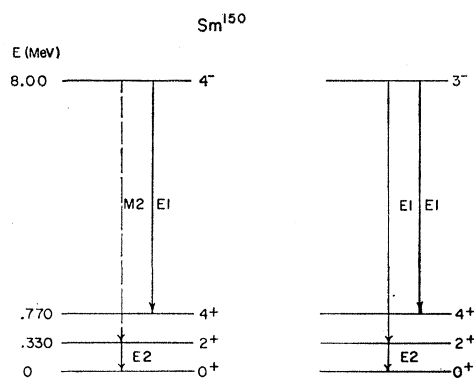


FIG. 8. The expected high-energy transitions to the first and second excited states of  $\text{Sm}^{150}$  after capture of a slow neutron. The energy of the neutron is negligible compared to the binding energy (8.00 MeV).

the transition to the second excited state ( $4^+$ ) is  $E1$ . On the basis of the binding energy (8.00 MeV), the transition energies from thermal capture level to the first excited state and to the second excited states are 7.67 and 7.23 MeV, respectively. The second transition (7.23 MeV) is seen in the thermal capture  $\gamma$ -ray spec-

trum,<sup>14</sup> whereas the first (7.67 MeV) is not.<sup>14,38</sup> This is consistent with the fact that most<sup>39</sup> of the thermal capture is due to the first resonance at 0.0976 eV which is  $4^-$ . The study of the capture  $\gamma$ -ray spectra should be extended to the higher energy resonances. On the basis of our spin assignments, the 7.23-MeV transition would be strongly favored over the 7.67-MeV transition in the case of the 0.87-, 4.93-, and 8.9-eV resonances of  $\text{Sm}^{149}$ .

#### ACKNOWLEDGMENTS

One of us (H. M.) would like to acknowledge several helpful discussions with Dr. E. Ambler, Dr. J. C. Eisenstein, Dr. J. F. Schooley, and Dr. R. I. Schermer. It is also a pleasure to acknowledge the help of Dr. Günter Brunhart, J. Roberge, and R. Comizzoli.

The technical assistance of R. Schmidt, J. Smolski, R. Smith, and E. Caruso is deeply appreciated. One of us (H. P.) would like to acknowledge the kind hospitality of Brookhaven National Laboratory during his temporary stay.

<sup>38</sup> N. Fiebiger (private communication).

<sup>39</sup> A recent abstract, R. D. MacFarlane and I. Almodovár, Bull. Am. Phys. Soc. 7, 334 (1962), indicates that a small amount of the thermal cross section might be  $3^-$ .